Dynamic Model Test and Analysis for a Prestressed Concrete Containment Vessel

Tsuneo Yamaguchi
Toshikazu Takeda

ABSTRACT

In order to get a reasonable prediction for dynamic behavior of the structure of prestressed concrete containment vessels for nuclear reactors (PCCV), an experiment was performed with a 1/10 scale PCCV model, mounted on the impact testing platform and subjected to the impact load.

The model, simulated to a prestressed concrete containment structure for 500 MWe PWR, consists of a prestressed concrete dome and cylinder, and a reinforced concrete slab. Moreover the morel is provided with a ring girder at the intersection of the dome and the cylinder, and six vertical buttresses in the cylinder.

A comparison between the test results and the calculation ones of the PCCV model was made in this paper, and a propriety of the dynamic analysis method was discussed, too. Both the measured and calculated results showed reasonable agreement with respect to response accelerations and strains.

The theoretical model for the dynamic analysis was constructed with consideration of rocking effects at the base, and the general equations derived were specialized to an idealized lumped-mass model.

1. INTRODUCTION

In the design of nuclear power plant structures, the safety margin is much required more than in the design of ordinary building structures. Especially, the dynamic behaviors of nuclear power plant buildings are connected with safety of mechanical system as well as the safety of itself. Therefore, in order to ensure the safety of nuclear power plant under strong earthquake motions, it is necessary to study in detail the dynamic behaviors of the building structures.

Although the prestressed concrete containment structure for nuclear power plant is essentially a very simple shape structure in concept, it can be said that there are still some problems in the dynamic analysis of the structure. Moreover, it has become necessary to consider the structure-foundation interaction effects on today's aseismic design of nuclear power plants.

There are a number of different types of PCCV structures which are in the process of being designed and constructed in foreign countries. The different types are essentially as follows:

1. Fully post-tensioned, using vertical tendons, hoop tendons anchored at vertical buttresses, and a triangular arrangement of dome tendons.
2. Fully post-tensioned, using opposing helical tendons anchored at the top and bottom of the cylinder and a triangular arrangement of dome tendons.
3. Post-tensioned only vertically, with mechanically spliced reinforcing steel in the hoop direction and in the dome.

In order to obtain aseismic design data for the PCCV structure of type 1, a dynamic test for a 1/10 scale model was performed, and the experimental results were compared with the calculated.

2. EXPERIMENTAL STUDY

2.1. Description of the Model

Fig. 1 shows the whole view of the PCCV model for the test. The model consists of a prestressed reinforced concrete cylindrical shell with a shallow dome, 4 m 550 in height, 3 m 300 in diameter and about 30 ton in weight. Its dimensions are on the order of one-tenth those of a full size prestressed concrete containment vessel for 500 MWe PWR. The configuration of the model is shown in Fig. 2.

The model was disigned for 4.2 kg/cm^2 internal pressure, which was representative value of pressure met in actual design pressure. The concrete of the model was maintained under compression which resulted in superior crack control. The unbonded prestressing system was primarily used for membrane stresses and the bonded reinforcing bar for secondary stresses.

The dimensions of the ring girder at the intersection of the dome and the cylinder were determined primarily to provide sufficient space and edge distance for the anchorage of the vertical and the dome tendons. The inside curvature of the ring girder provides a smooth transition for membrane stress flowing from the dome to the cylinder.

The arrangements of the tendons and reinforcing bars are shown in Fig. 2, too. The tendon system for the dome consists of three equal groups, oriented at 120° to each other. The tendons in each group run across the dome in parallel vertical planes.

The cylinder was prestressed with the hoop and the vertical tendons. Each hoop tendon which covered 120° of circumference was anchored at the vertical buttresses. Six buttresses were provided in the cylinder.

The unbonded tendons consisted of conventional stressteel bar (12,500 kg/cm^2 yield strength) and anchored at both ends. The yield strength of the bonded reinforcing bars, used at the base slab, the cylinder and the dome, was 3,250 kg/cm^2, and concrete with uniaxial compressive strength of 450 kg/cm^2 was used.

The model was prestressed with the tendons so as to be about 30 kg/cm^2 meridional membrane stress. The calculated displacement values of the model subjected to the full prestressing force is shown in Fig. 3.

2.2. Apparatus used for the Impact Load Test

Outline of the apparatus used for the test is shown in Fig. 4.

The apparatus was primarily planned to give the dynamic external disturbance to the base of a structural model, to the extent of its failure, in order to study the restoring force characteristics and damping. As the apparatus is comparatively large in scale and has large potential energy, such a large size structure as the 1/10 scale PCCV model can be tested dynamically, too.

The impact is produced by the collision of the test platform and the pendulum. The accelerations and the duration time of the impulse wave on the test platform can be changed arbitrarily, because of the five springs made of artificial rubber and steel plates are provided at one side of the platform against which the pendulum is collided.

Test Procedure

This impact load test was conducted at follows;

At first, the model was fixed on the test platform with 12 steel blocks and anchor bolts, and the impact load was applied at the bottom of the model.

Although a series of the tests were repeated with various height of the pendulum, the test results, with 3,000 m in height of the pendulum, were presented in this paper.

As shown in Figs. 5, 6, 7, the accelerograms and the strain records at various positions of the model were measured during the test.

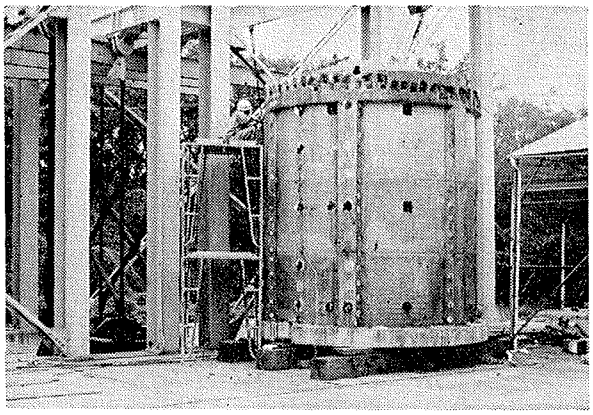

Fig-1 Outline of PCCV Model

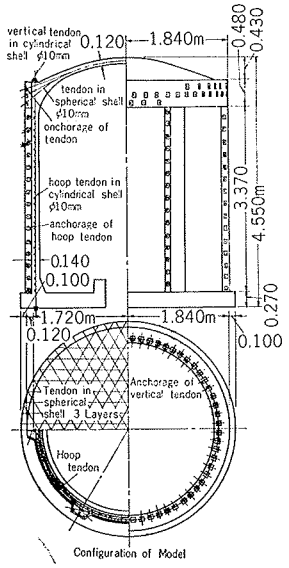

Fig-2 Configuration of PCCV Model

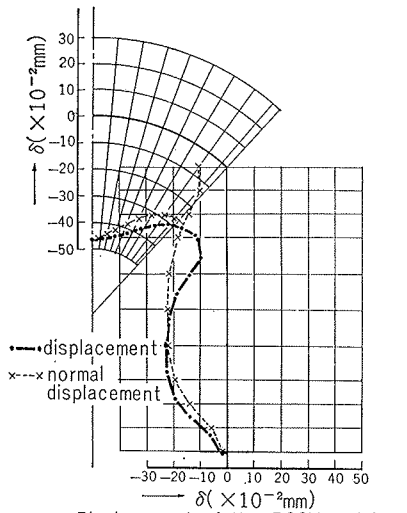

Displacement of the PCCV model subjected to full prestressing force

Fig-3

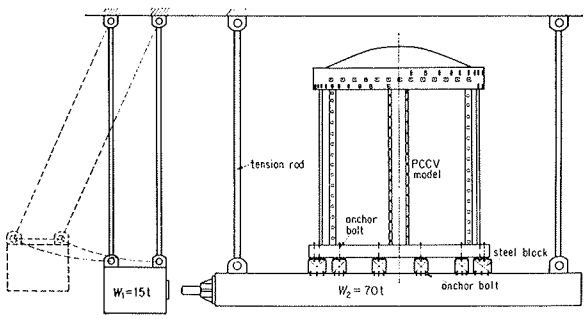

Fig-4 Apparatus of impact load test

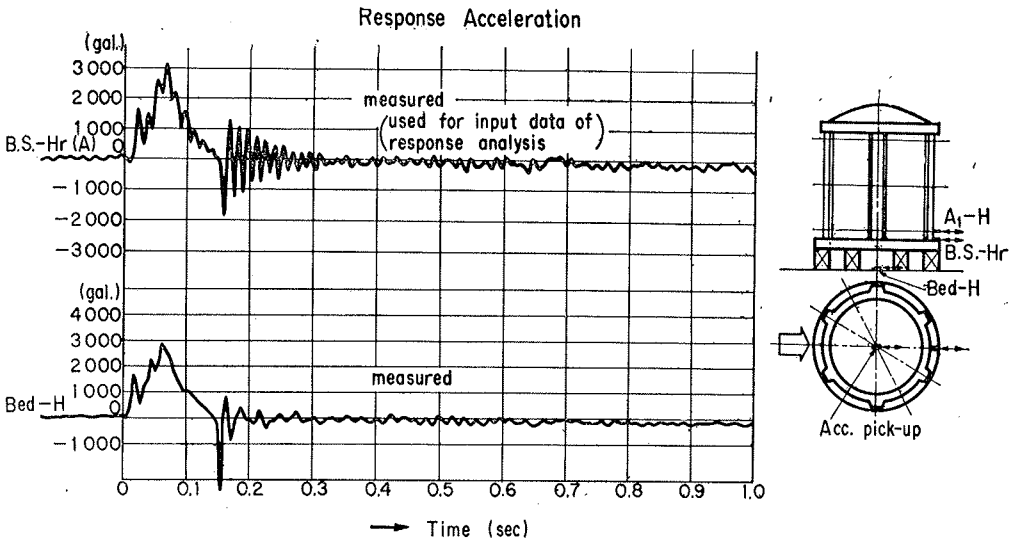

Fig-5-1 Measured Accelerations on the Base Slab and the Test Bed

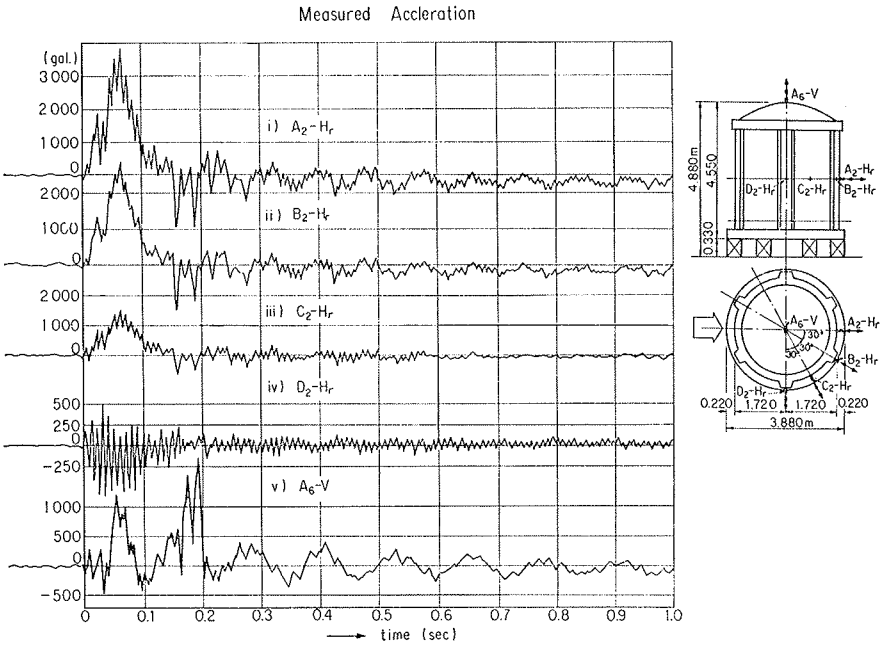

Fig-5-2 Measured Acceleration

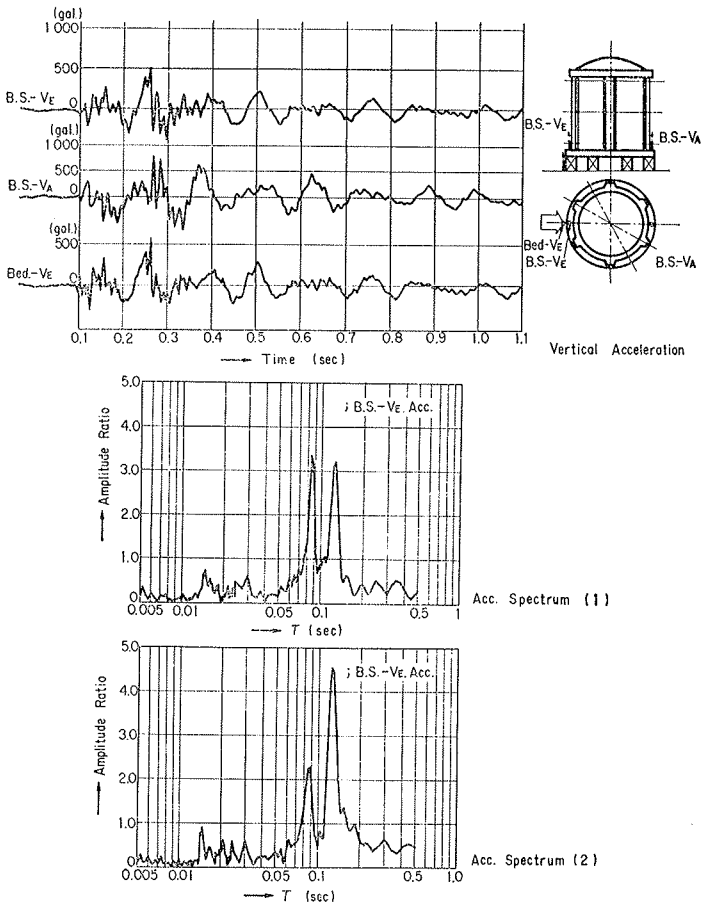

Fig-6 Measured Acceleration

2.3. Test Results

Accelerograms of the Platform and the Base Slab of the Model:

As shown in Fig. 5-1, the waveform of horizontal acceleration at center on the platform was approximately a half cycle of sine, the duration time of which was about 0.15 sec., and the maximum acceleration obtained was about 2,900 gal. Because of the swing motion of the platform after the collision, the acceleration with rather longer natural period was observed in the accelerogram. That natural period was about 5.0 sec., and the second collision occurred at 2.5 sec. after the first one.

Accelerogram of the base slab of the model is almost similar to that of the platform, but there were some differences in the term followed by a half cycle of strong impulse, and the maximum acceleration on the base slab was about 3,100 gal.

Accelerograms of the Cylinder and the Dome

The measured horizontal accelerograms along the vertical plane, A-section are shown in Figs. 10. The response acceleration at A_1-section, 30 cm apart from the base, was similar to that of the base slab. It seemed that the difference between the accelerograms of the base slab and the others was enlarged, as the distance from the base become long. The accelerogram of the top of the model, A_6-section, showed a marked periodicity at the portion of free vibration. In addition, the features were similar to those of the vertical accelerograms of the base slab and the platform.

The measured horizontal accelerograms of the cylinder at the same level in radial direction are shown in Fig. 5-2. As shown in it, the features of the wave forms are almost all the same except in the direction perpendicular to the external force (D_2-H_r). For example, the maximum values of each acceleration were attained simultaneously, and the other peak values, too. The proportions of the maximum ones in three directions (A_2-H_r, B_2-H_r, C_2-H_r) are about 1:0.76:0.4, and the effects of the circumferential modes were not observed clearly.

Vertical Accelerograms of the Base Slab and the Platform

The measured vertical accelerograms of the base slab and the platform are shown in Fig. 6-1, and the fourier spectrums of the accelerations for B.S.-V_A and B.S.-V_E are shown in Figs. 6-2, 3.

The measured vertical accelerations in these figures shows a remarkable rocking vibration of the system and the natural period of the rocking vibration is between 0.085 and 0.125 sec.

Strains of the Model

The measured response strains at the position of A_1-section are shown in Fig. 7. The maximum strain of about 50×10^{-6} was recorded on the outer surface in the meridional direction. While, the maximum strain on the inner surface of concrete was about 25×10^{-6}. The axial strain and the bending strain in A_1-section result in $\varepsilon_N \approx 38\times10^{-6}$, $\varepsilon_M \approx 13\times10^{-6}$, respectively. On the other hand, the the hoop strains were much smaller than that.

3. ANALYTICAL APPROACH

3.1. Idealization of the Model

The PCCV model was idealized with the 7 lumped-mass model, (Fig. 8-1), in dynamic analysis, and the finite element technique for axisymmetrical shell subjected to asymmetrical load was used in the calculation of the softness coefficient matrix.

The idealization of the structure for the F.E.M. is shown in Fig. 8-2; the structure of the model is represented by triangular ring elements which is divided into 7 segments. The radial and the circumferential components of the horizontal unit load were applied on the nodes in each segment of the idealized structure. In order to simplify the calculation, the load distribution in horizontal

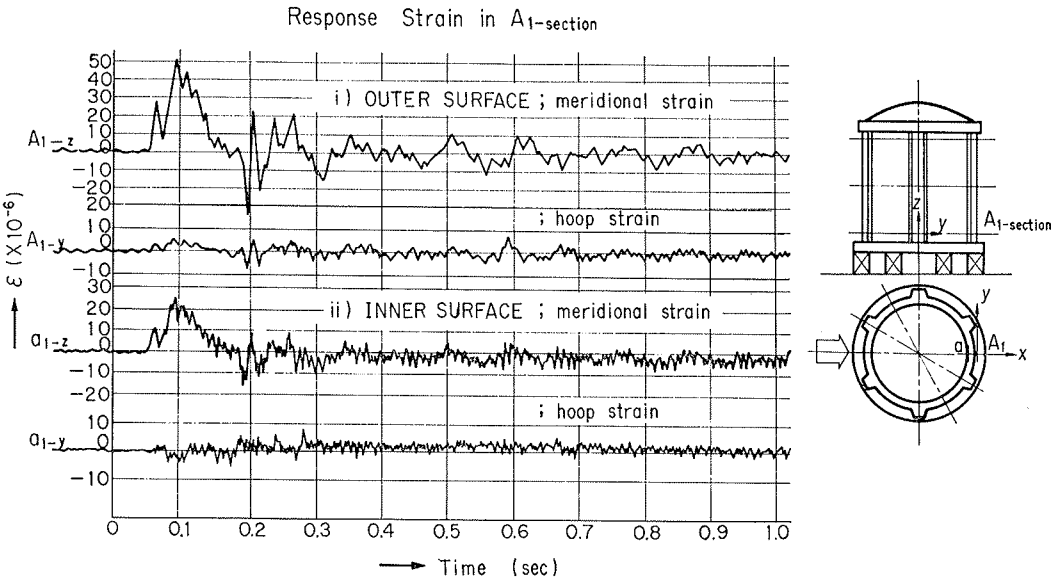

Fig-7 Measured Strain

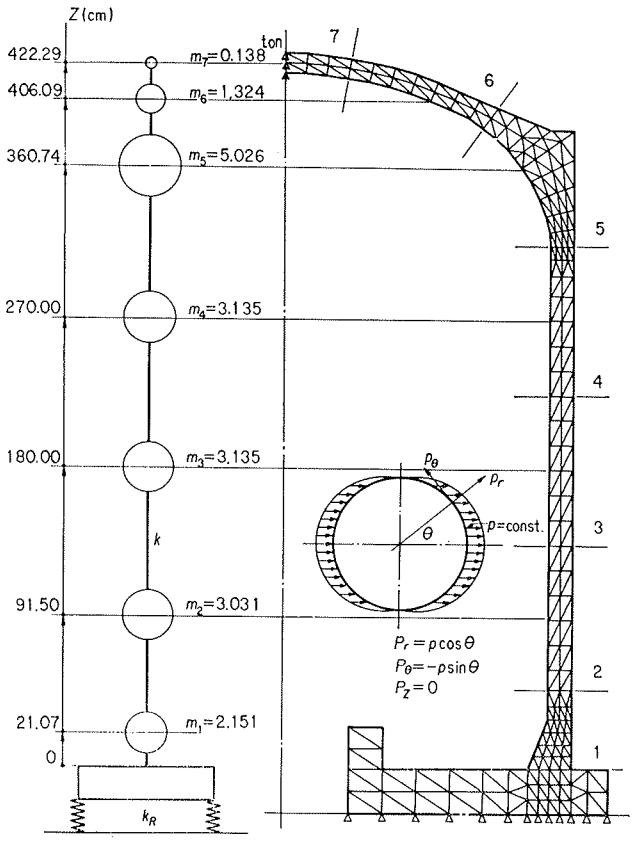

Fig-8 Idearization of the Model

plane was assumed as shown in Fig. 8-2, while, the one in vertical plane was proportioned to masses of the ring elements.

The horizontal displacements of the model subjected to the unit load 1 ton are listed in Table I, the values of which are evaluated with the F.E.M. and the beam theory, respectively. Though there are some difference between those values, it would be convenient to use the beam theory for approximation.

; ①FEM, ②Beam Theory with Vertical Buttresses, ③Beam Theory with No Buttress.

		1		2		3		4		5		6		7	
		P_1		P_2		P_3		P_4		P_5		P_6		P_7	
δ_1	①	0.1230−04	1.0												
	②	0.185 −04	1.50												
	③	0.216 −04	1.76												
δ_2	①	0.2081−04	1.0	0.8341−04	1.0										
	②	0.188 −04	0.90	0.851 −04	1.02										
	③	0.220 −04	1.06	0.996 −04	1.19										
δ_3	①	0.2327−04	1.0	0.1095−03	1.0	0.2129−03	1.0								
	②	0.192 −04	0.83	0.0920−03	0.84	0.1963−03	0.92								
	③	0.225 −04	0.97	0.1085−03	0.99	0.2306−03	1.08								
δ_4	①	0.2459−04	1.0	0.1188−03	1.0	0.2564−03	1.0	0.3916−03	1.0						
	②	0.196 −04	0.80	0.1001−03	0.84	0.2257−03	0.88	0.3706−03	0.95						
	③	0.230 −04	0.94	0.1175−03	0.99	0.2656−03	1.04	0.4335−03	1.11						
δ_5	①	0.2606−04	1.0	0.1285−03	1.0	0.2849−03	1.0	0.4676−03	1.0	0.6426−03	1.0				
	②	0.200 −04	0.77	0.1077−03	0.84	0.2552−03	0.90	0.4371−03	0.93	0.6298−03	0.98				
	③	0.234 −04	0.90	0.1267−03	0.99	0.3010−03	1.06	0.5131−03	1.10	0.7446−03	1.16				
δ_6	①	0.2680−04	1.0	0.1333−03	1.0	0.2991−03	1.0	0.4985−03	1.0	0.7087−03	1.0	0.8348−03	1.0		
	②	0.202 −04	0.75	0.1116−03	0.84	0.2700−03	0.90	0.4704−03	0.94	0.6893−03	0.97	0.8039−03	0.96		
	③	0.237 −04	0.88	0.1313−03	0.98	0.3187−03	1.07	0.5529−03	1.11	0.8157−03	1.15	0.9518−03	1.14		
δ_7	①	0.2713−04	1.0	0.1351−03	1.0	0.3042−03	1.0	0.5095−03	1.0	0.7308−03	1.0	0.8763−03	1.0	0.1002−02	1.0
	②	0.203 −04	0.75	0.1135−03	0.84	0.2753−03	0.90	0.4796−03	0.94	0.7106−03	0.97	0.8307−03	0.95	0.8740−03	0.87
	③	0.238 −04	0.88	0.1336−03	0.99	0.3250−03	1.07	0.5671−03	1.11	0.8413−03	1.15	0.9839−03	1.12	0.1035−02	1.03

Table-I Softness Coefficient Matrix for Unit Load (P=1ton)

In this dynamic analysis, the base slab of the model was assumed to be rigid and to be supported with a rotational spring. The spring constant K_R was derived with the rocking period, 0.1 sec., of the vibrational system.

3.2. Analysis Method

In order to simplify the dynamic analysis, the general equations derived were specialized to an idealized lumped-mass system with the rotational spring at the base as shown in Fig. 8-1.

The equation of motion of the model structure subjected to the horizontal force takes the form,

$$[m]\{\ddot{Y}\} + [C]\{\dot{Y}\} + [K]\{Y\} = \{f(t)\} \quad \cdots\cdots\cdots\cdots \quad (1)$$

in which [m] = mass matrix, [C] = damping matrix, [K] = stiffness matrix, {Y} = displacement vector, and {f(t)} = forcing vector.

The mass matrix [m] is a diagonal matrix

$$[m] = \begin{bmatrix} I & & & & \\ & m_0 & & 0 & \\ & & m_1 & & \\ & & & \ddots & \\ & & & & m_i \\ & & & \ddots & \\ & 0 & & & m_n \end{bmatrix} \quad \cdots\cdots\cdots\cdots \quad (2)$$

in which I = moment of inertia of the system, m_0 = base mass, and m_i = mass of the i^{th} segment.

The stiffness matrix is

$$[K] = \begin{bmatrix} 1/K_R & 0 & H_j/K_R \\ 0 & 1/K_H & 1/K_H \\ H_i/K_R & 1/K_H & \alpha_{ij} + H_iH_j/K_R + 1/K_H \end{bmatrix}^{-1} \quad \cdots\cdots\cdots\cdots \quad (3)$$

in which α_{ij} = coefficient of the softness matrix of the superstructure fixed on the base, K_R = rotational spring constant at the base, K_H = translational spring constant at the base (swaying spring const.), and H_i = height of the i^{th} mass level above the base.

The damping matrix is

$$[C] = \begin{bmatrix} 1/C_R & 0 & H_j/C_R \\ 0 & 1/C_H & 1/C_H \\ H_i/C_R & 1/C_H & [C_0]^{-1} + H_iH_j/C_R + 1/C_H \end{bmatrix}^{-1} \quad \cdots\cdots\cdots\cdots \quad (4)$$

in which $C_R = r_R\mathbf{K}_R$, $C_H = r_HK_H$, $[C_0] = [T]^t[r_i\overline{K}_{ij}][T]$

r_R = internal viscous damping coefficient of the rotational spring,
r_H = internal viscous damping coefficient of the translational spring,
r_i = internal viscous damping coefficient of the superstructure,
$[T]$ = displacement transformation matrix,

and

$[\overline{K}_{ij}]$ = stiffness matrix of the superstructure in the local coordinate.

The relation between r and damping factor h may be given as follows:

$$\left.\begin{aligned} r_R &= T_1h_R/\pi \\ r_H &= T_1h_H/\pi \\ r_i &= T_1h_i/\pi \end{aligned}\right\} \quad \cdots\cdots\cdots\cdots \quad (5)$$

in which T_1 = fundamental natural period, h_R = damping factor of the rotational spring, h_H = damping factor of the translational spring, and h_i = damping factor of the superstructure.

Let the displacement vector be

$$\{Y\} = \begin{Bmatrix} 0 \\ Y_0 \\ Y_1 \\ \cdot \\ \cdot \\ \cdot \\ Y_i \\ \cdot \\ \cdot \\ \cdot \\ Y_n \end{Bmatrix} \quad \cdots\cdots\cdots\cdots \quad (6)$$

and the forcing vector be

$$\{f(t)\} = \begin{Bmatrix} 0 \\ f_0(t) \\ f_1(t) \\ \cdot \\ \cdot \\ \cdot \\ f_i(t) \\ \cdot \\ \cdot \\ \cdot \\ f_n(t) \end{Bmatrix} \qquad \cdots\cdots\cdots\cdots \quad (7)$$

3.3. Calculated Results

The calculated natural periods for the model are listed in Table II, in which the rotational spring constant was derived with consideration of the rotational stiffness for the vibrational system. The period of rocking vibration was calculated with the relation between the moment of inertia and the rotation.

The fundamental period for the fixed condition is a few longer than the second natural period for the condition with the rotational spring, because the second mode has the counter phase in the rotation. Moreover, in the condition with the rotational spring, the fundamental period of the system is 9 times as much as the second period. It results that the first mode vibration is quite predominant, because the duration time of the impulse at the base is far longer than the fundamental period.

	ROCKING SPRING K^R 1.151×10^7 t·cm	FIXED
1 st MODE	0.1005sec	
2 nd MODE	0.0112	0.0156sec
3 rd MODE	0.0041	0.0041
4 th MODE	0.0020	0.0020
5 th MODE	0.0014	0.0014
6 th MODE	0.0011	0.0011
7 th MODE	0.0007	0.0007
8 th MODE	0.0006	0.0006

Table-II Calculated Period for the PCCV Model

The vibrational modes of the 7-lumped-mass model are shown in Fig. 9, and the excitation functions are listed in Table III. The calculated response accelerations of each mass under the base motion are shown in Fig. 10.

In the analysis, the response accelerations in three cases were calculated, and shown in Fig. 10-1, ii). In each case, the damping factors were assumed as follows;

	damping factor	
	superstructure	rotational spring
case 1	0.03	0
2	0.05	0
3	0.02	0.05

	1 st	2 nd	3 rd	4 th	5 th	6 th	7 th	8 th
7	0.68675	0.67466	−0.55254	0.42643	−0.43063	0.22207	−0.02193	−0.00481
6	0.66127	0.65496	−0.46169	0.28847	−0.23099	0.09176	−0.00457	0.00080
5	0.59000	0.59928	−0.21876	−0.01256	0.10372	−0.06938	0.00779	−0.00009
4	0.44697	0.45377	0.27634	−0.27297	−0.00150	0.12831	−0.03095	0.00003
3	0.30465	0.27195	0.58603	0.01178	−0.13476	−0.11209	0.07244	−0.00001
2	0.16481	0.10464	0.44828	0.28275	0.12583	0.05702	−0.18334	0.00000
1	0.05386	0.00252	0.11386	0.10205	0.07277	0.05717	0.59778	0.00000
0	0.00154	−0.00147	−0.00003	−0.00002	−0.00000	−0.00000	−0.00001	−0.00000

Table-III Excitation Functions (kr = 1.151×10^7 t-cm)

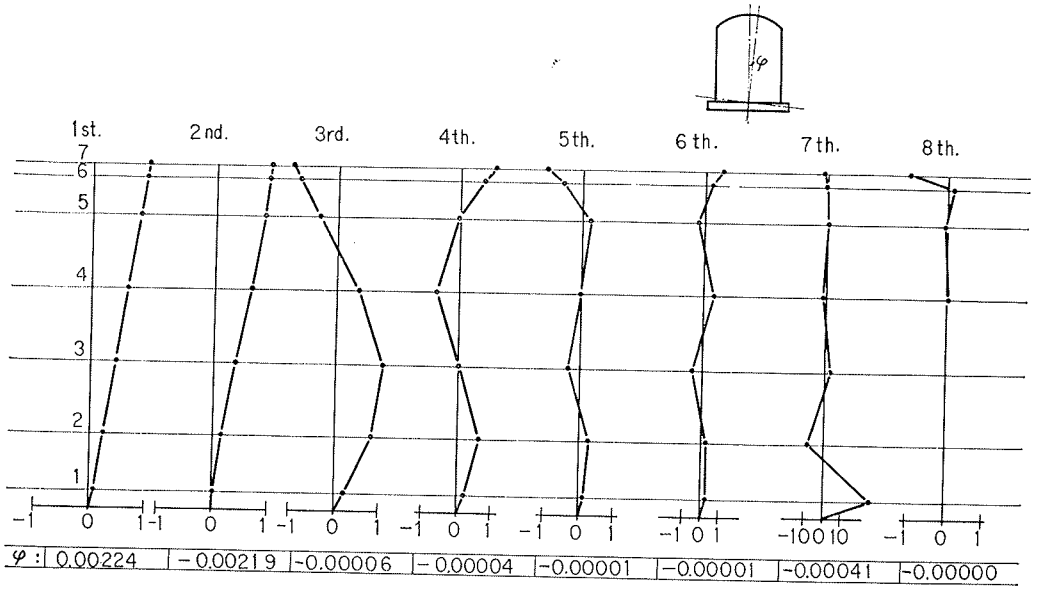

Vibrational Mode

Fig-9

In the other figures and tables, only the results of case 1 are shown.

Fig. 11 shows the displacements and the shearing forces when the top mass displacement reached at the maximum value, in which (i) is the relative displacement to the base, (ii) is the structural deflection, that is the relative displacement subtracted by the rotational displacement, and (iii) is the shearing force diagram.

As shown in this figure, it is seen that the deflection of the structure itself is much smaller than the relative displacements.

The strain histories at the A_1-section are shown in Fig. 12. When the relative displacement, the structural deflection of the top and the base shearing force reached at the maximum value respectively, the strains are as follows:

		at max. relative displacement	at max. deflection	at max. base shear
	time	0.080 sec.	0.095 sec.	0.110 sec.
on the inner surface;				
circumferential strain	ε_y	3.9×10^{-6}	1.6×10^{-6}	1.4×10^{-6}
meridional strain	ε_z	18.1	38.0	37.8
on the outer surface;				
circumferential strain	ε_y	5.8	5.3	2.5
meridional strain	ε_z	36.1	44.9	32.1

4. COMPARISON BETWEEN THE TEST AND THE CALCULATED RESULTS

The measured and the calculated accelerations are shown in Fig. 10. Although the response accelerations are not predicted precisely by the calculation, it can be said that overall response has been predicted. The first mode vibration, the rocking motion, is predominant in the response acceleration. The differences between both results are mainly due to the difference of the estimation of the rocking characteristics at the base.

As before-mentioned, the maximum strain was measured on the outer surface of the A_1-section, in the meridional direction, and the value was about $\varepsilon z = 50 \times 60^{-6}$. On the other hand, the

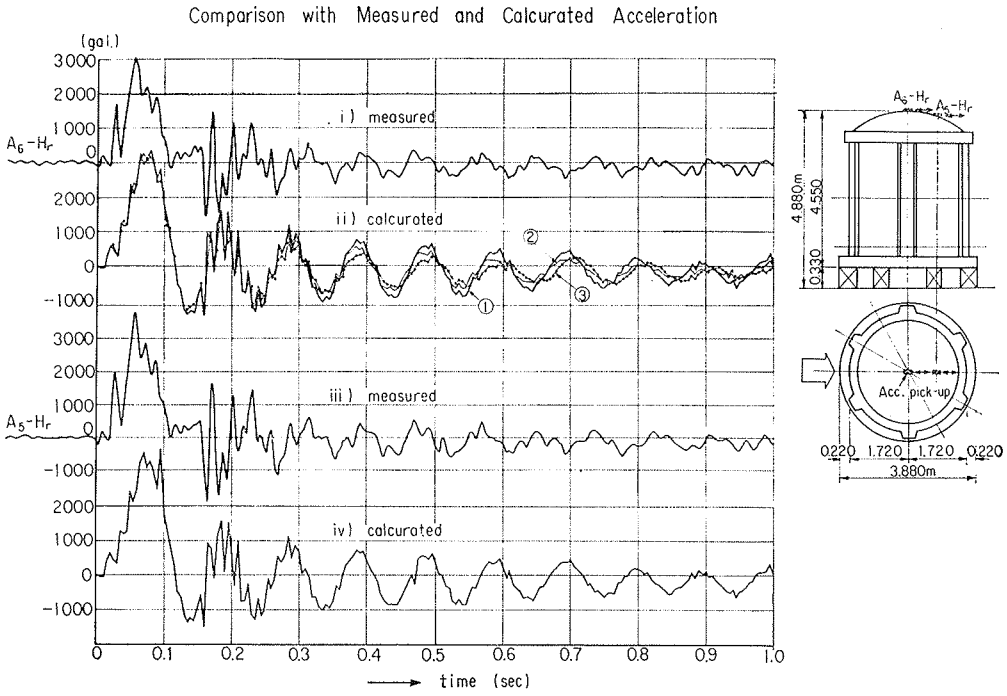

Fig-10-1

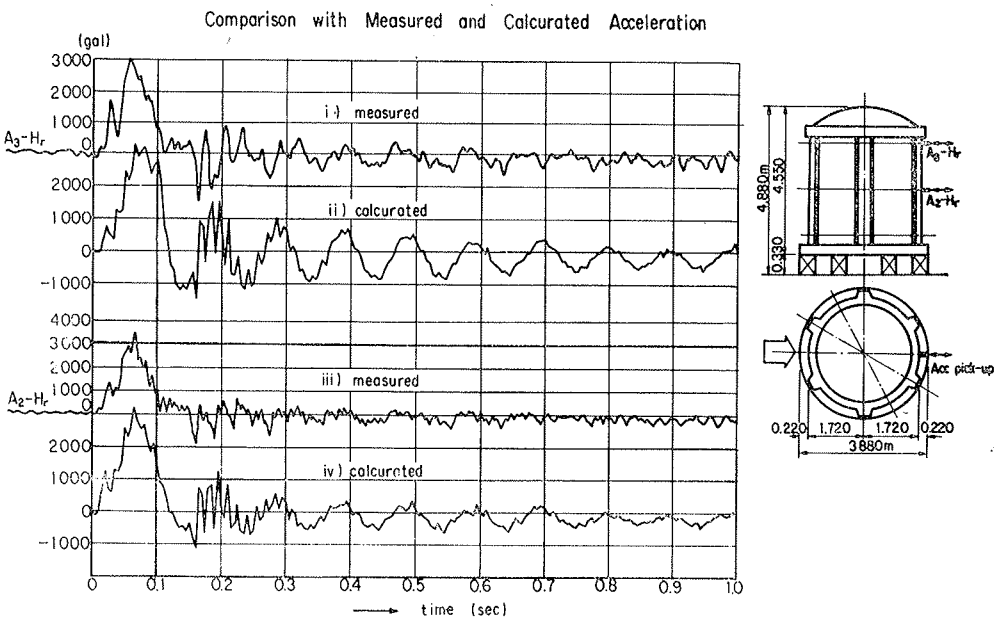

Fig-10-2

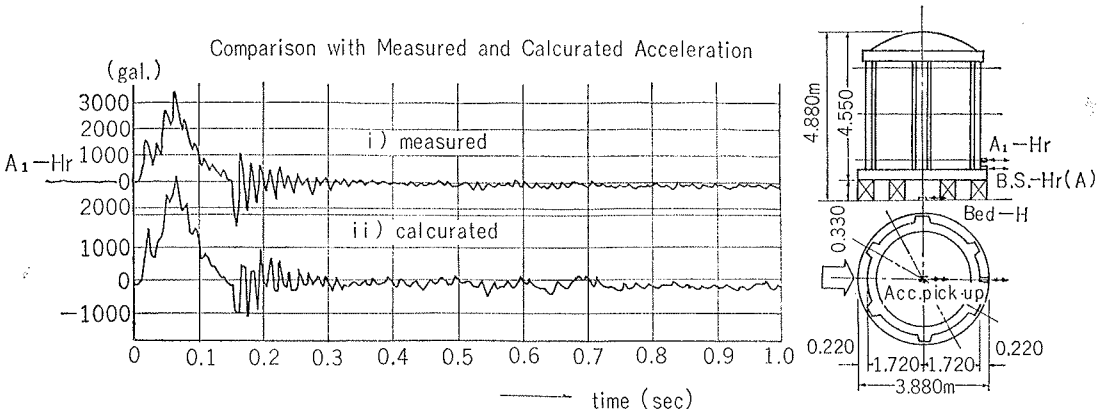

Fig-10-3

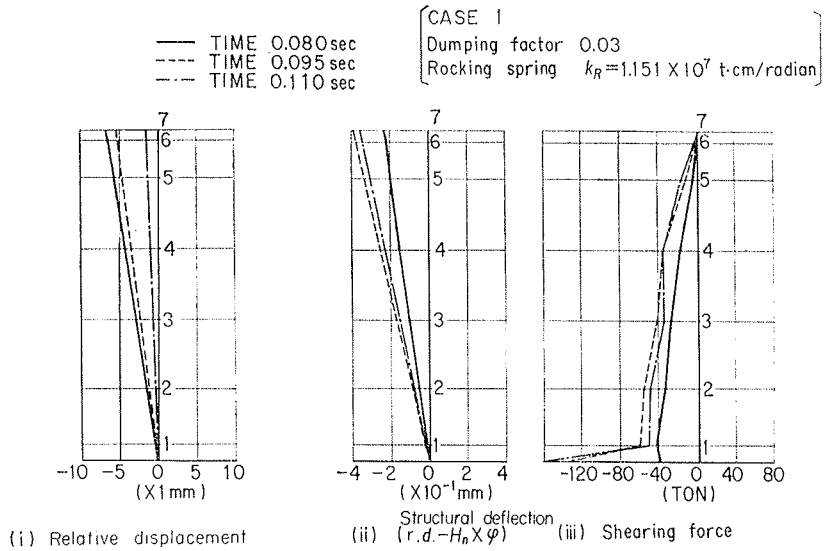

Maximum displacement and shearing force ; response analysis considering rocking spring k_R

Fig-11

calculated strain was 45×10^{-6} at the same position when the deflection of the model structure itself was reached at the maximum value. As shown in Fig. 12, the time at the maximum response strain is about 0.095 sec. after the first collision, which is recognized to be good agreement with the measured.

This may be another indication of adaptability of the calculation technique for the dynamic response analysis.

5. CONCLUSION

The 1/10 scale model for the PCCV was tested dynamically, to be subjected to the impulse at the base, the maximum acceleration of which is about 3,100 gal, and the dynamic analysis was made in due consideration of the rocking vibration effects.

The following conclusions can be drawn on the basis of both the test and the calculated results;

1) The maximum response acceleration was about 3,700 gal which was measured at the position of the A_5-section of the PCCV model. So, the response magnification was about 1.2. The

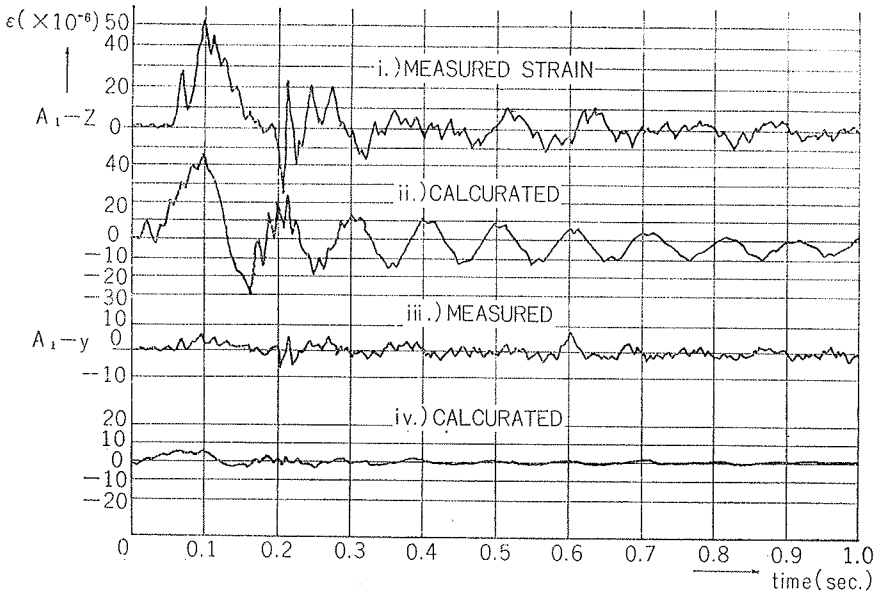

Fig-12-1

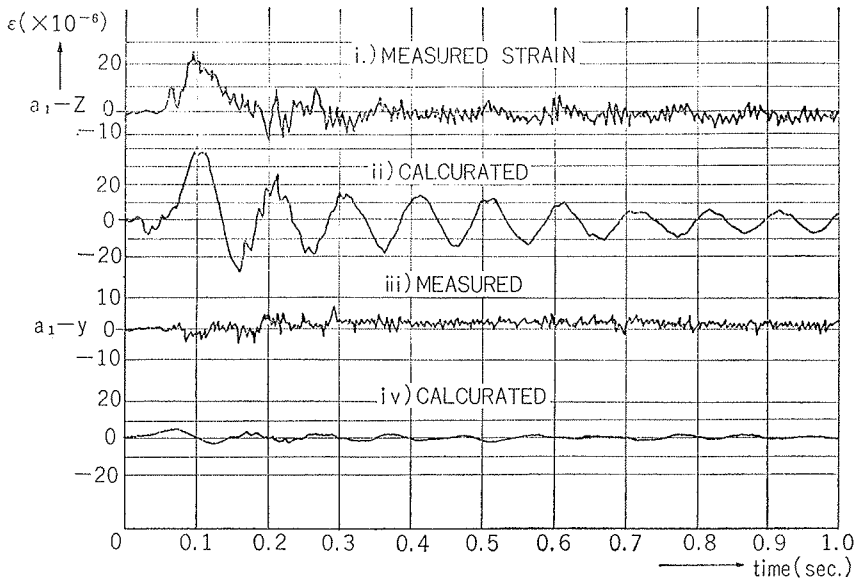

Fig-12-2

maximum stress of the model measured was about 15 kg/cm², the value of which was in good agreement with the calculated value, and no concrete crack in the model was observed in spite of numbers of tests repeated.

2) As shown in Figs. 10, 12, though the lumped-mass system was used for the dynamic analysis, the comparison between the measured and calculated results shows reasonable agreement with respect to response accelerations and strains.

3) When the model will be developed into the full scale, the foundamental period of the PCCV structure is about 0.112 sec.

As a PCCV structure, in general, is provided with very large stiffnesses, masses and moments of inertia, the soil-structure dynamic interaction effects cannot be neglected in the dynamic analysis. Especially in future, it seems that the detailed dynamic analysis for the interaction problems may be required.

Reference

1. Grafton, P.E. and Strome, D.R., "Analysis of Axisymmetrical Shells by the Direct Stiffness Method", A/AA Journal, Vol. 1, No. 10, Oct. 1963.
2. Zienkiewicz, O.C. and Cheung, Y.K., "The Finite Element Method in Structural and Continum Mechanics", McGraw-Hill, 1967.
3. KAWAMATA, S. and SHIOYA, S., "A Stiffness Matrix for Unsymmetrical Problems of Solids of Revolution", SEISAN-KENKYU of Monthly Journal of Institute of Industrial Science, University of Tokyo, Vol. 20, No. 1, Jan. 1968.
4. KAWAMATA, S., "Stress Analysis of Axisymmetric Solids by the Finite Element Method", SEISAN-KENKYU of Monthly Journal of Institute of Industrial Science, University of Tokyo, Vol. 20, No. 5, May 1968.
5. Wahl, H.W. and Kulka, F., "American Practices in the Design of Prestressed Concrete Containment Structures" PCI Journal, June 1968.
6. Parmelee, R.A., "Building-Foundation Interaction Effects", Journal of the Engineering Mechanics Division, ASCE, EM2, April 1967.
7. Tajimi, H., Discussion of Ref. 6., Journal of the Engineering Mechanics Division, ASCE, EM6, Dec. 1967.
8. Kanai, K., Tajimi, H. and Kobayashi H., "Earthquake Engineering", KENCHIKU-KOZOGAKU-TAIKEI, Vol. 1, SHOKOKU-SHA, 1968, in Japanese.
9. Muto, K., Uchida, K. and Takase, H., "Studies on Aseismic Design for Nuclear Power Plants", Proceeding of 15th National Symposium on Bridge and Structural Engineering, Feb. 1970.